

Supporting Information

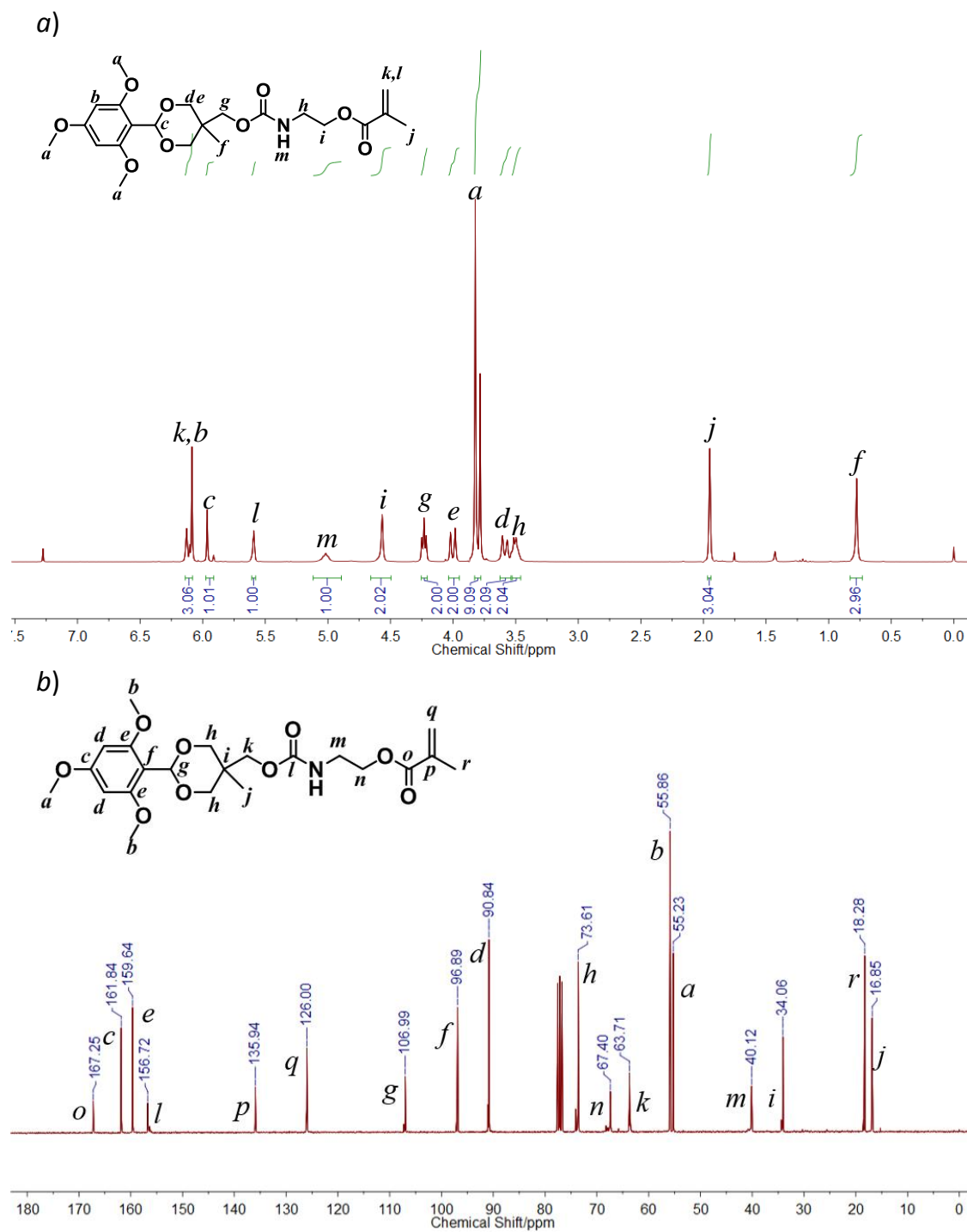
Acid-Disintegratable Polymersomes of pH-Responsive Amphiphilic Diblock Copolymers for Intracellular Drug Delivery

Lei Wang, Guhuan Liu, Xiaorui Wang, Jinming Hu,* Guoying Zhang,* and Shiyong
Liu*

*CAS Key Laboratory of Soft Matter Chemistry, Hefei National Laboratory for Physical
Sciences at the Microscale, iChem (Collaborative Innovation Center of Chemistry for
Energy Materials), Department of Polymer Science and Engineering, University of Science
and Technology of China, Hefei, Anhui 230026, China.*

* To whom the correspondence should be addressed.

E-mail: sliu@ustc.edu.cn (S.L.); hjm85@mail.ustc.edu.cn (J.H.); gy Zhang@ustc.edu.cn
(G.Z.)



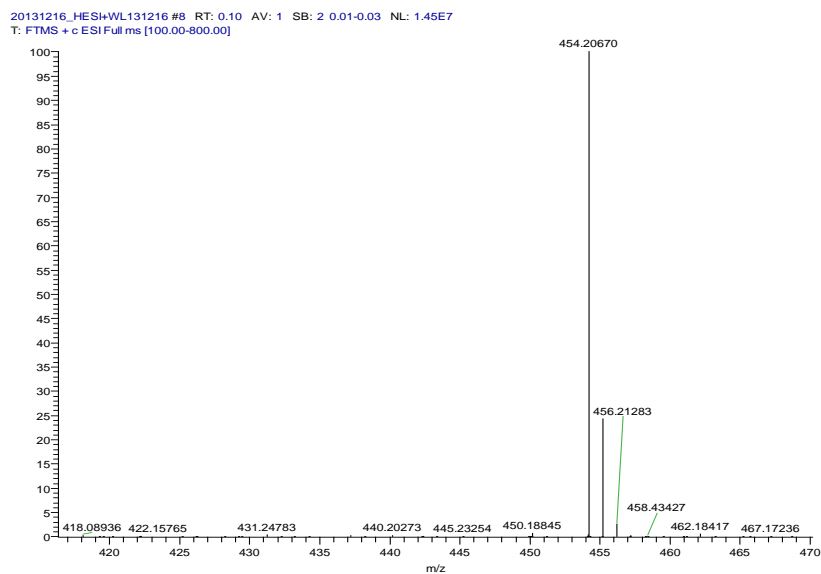


Figure S2. ESI-MS spectrum recorded for TTAMA monomer.

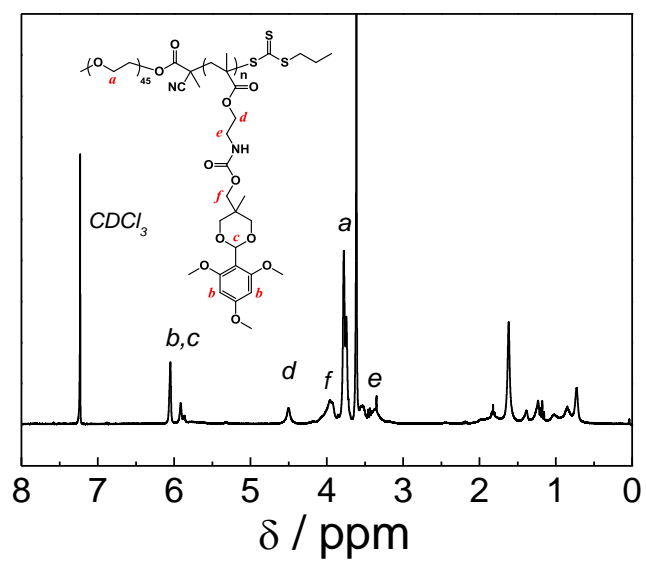


Figure S3. ^1H NMR spectrum recorded in CDCl_3 for **BP2** diblock copolymer.

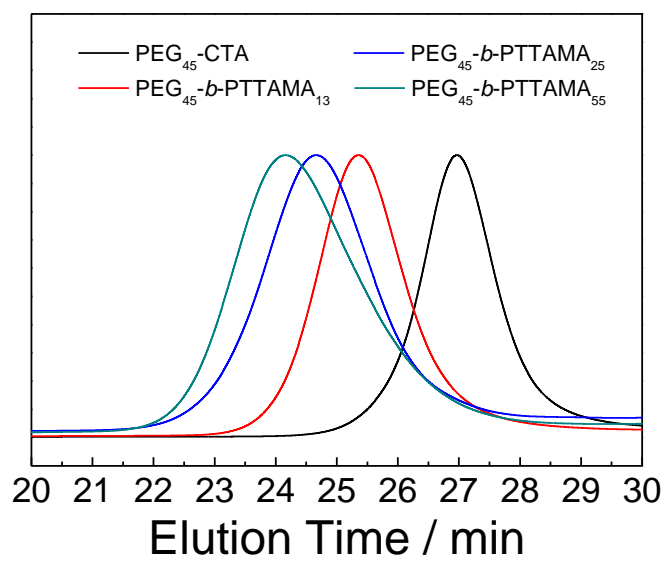


Figure S4. GPC traces of PEO-based macroRAFT agent (PEO₄₅-CTA) and **BP1-BP3** diblock copolymers, respectively.

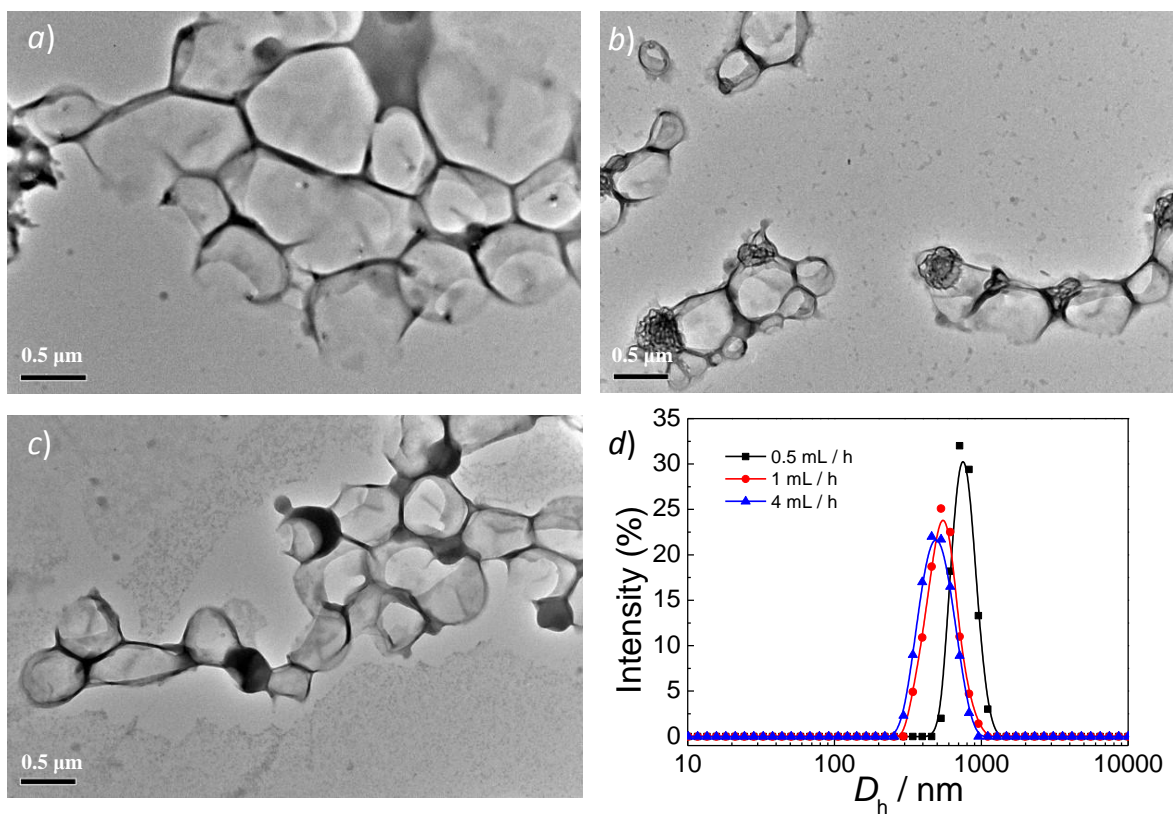


Figure S5. (a-c) TEM images of **BP2** polymersomes and (d) the corresponding intensity average hydrodynamic diameter distributions, $f(D_h)$, obtained at varying water addition rates: (a) 0.5 mL/h, (b) 1 mL/h, and (c) 4 mL/h.

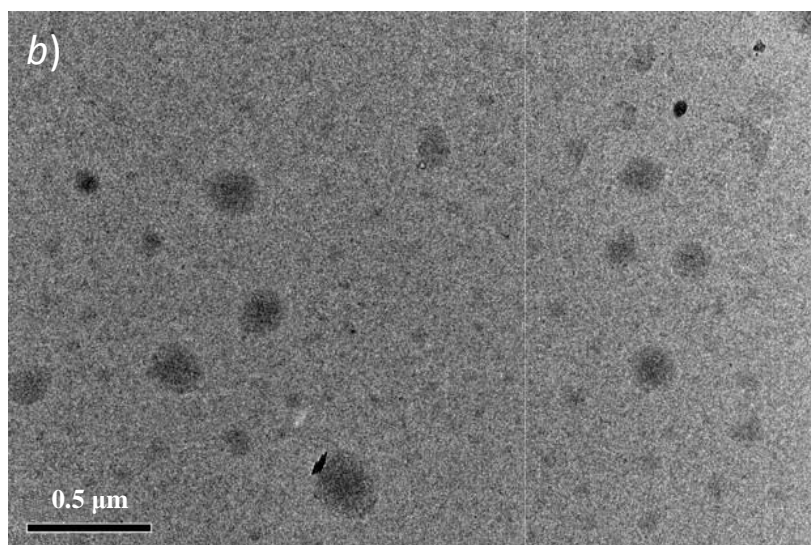
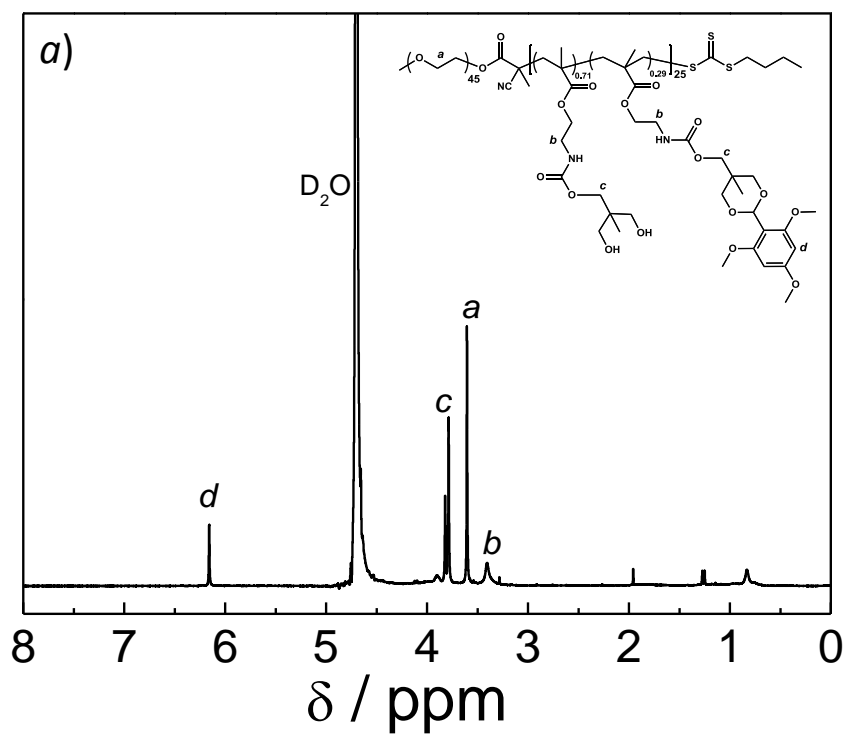


Figure S6. (a) ^1H NMR spectrum in D_2O and (b) typical TEM image recorded for **BP2** polymersomes after 5 days of hydrolysis in pH 5.0 buffer.

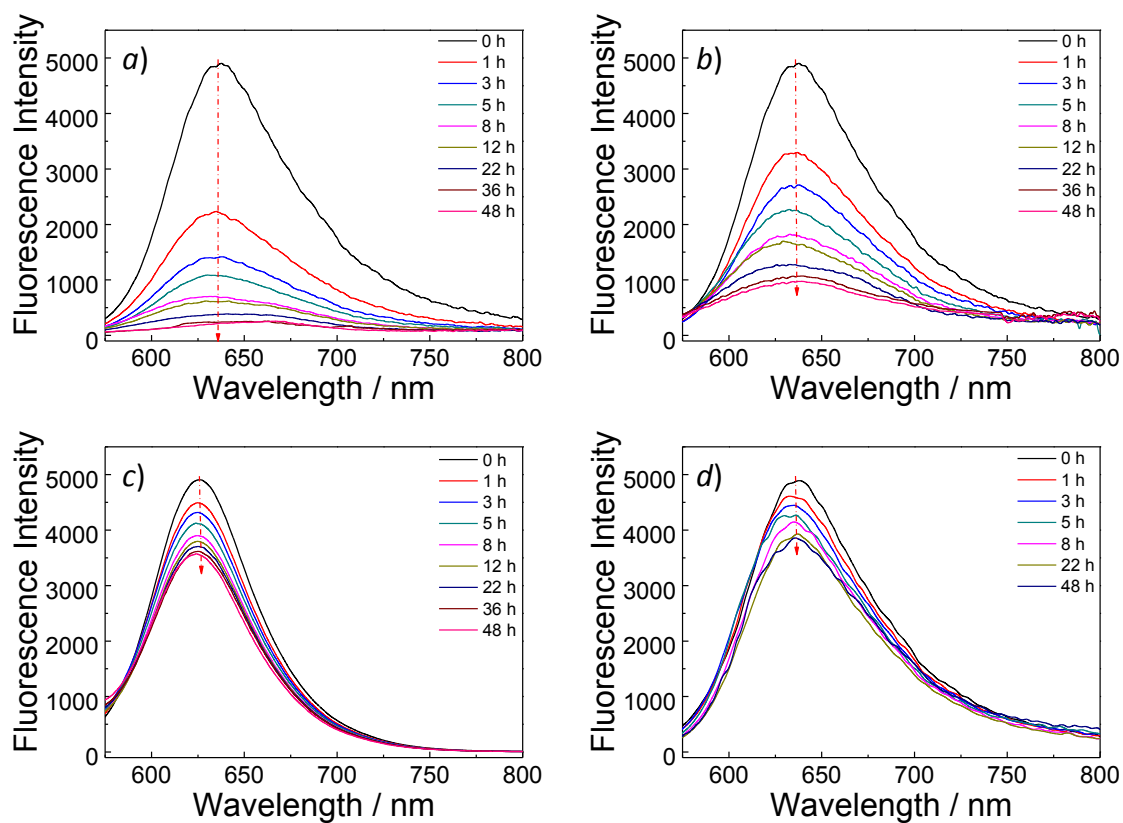


Figure S7. Release profiles of loaded Nile red from the hydrophobic bilayers of **BP2** polymersomes at varying pH: (a) 4.5, (b) 5.0, (c) 6.0, and (d) 7.4, respectively ($\lambda_{\text{ex}} = 550$ nm).

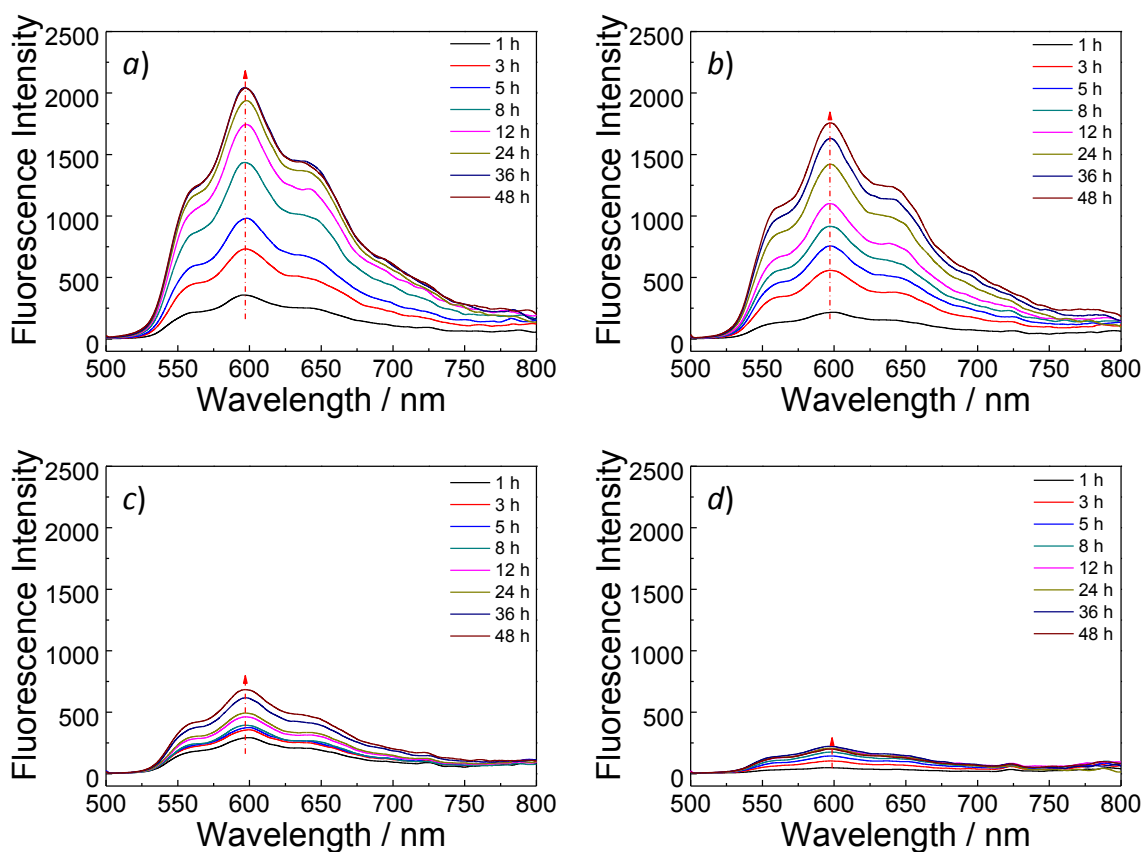


Figure S8. Release profiles of encapsulated DOX·HCl from the aqueous interiors of **BP2** polymersomes at varying pH: (a) 4.5, (b) 5.0, (c) 6.0, and (d) 7.4, respectively ($\lambda_{\text{ex}} = 480$ nm).

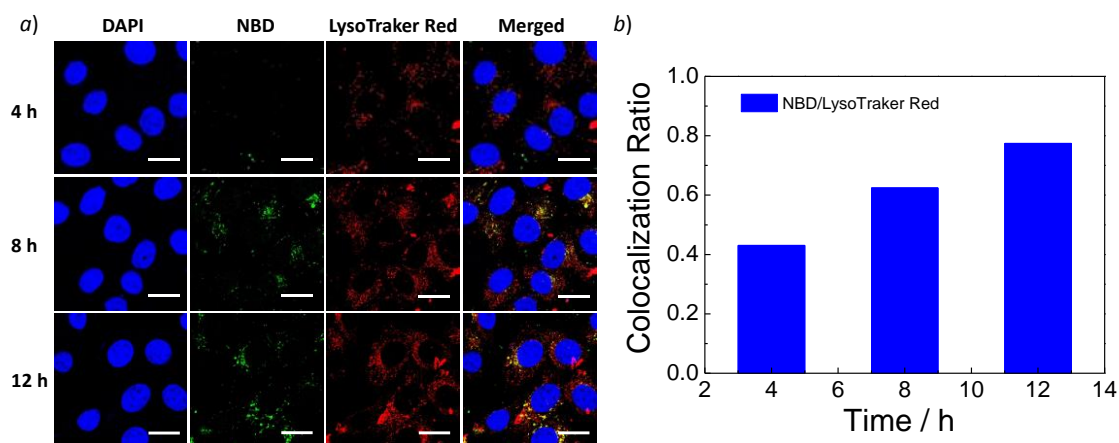


Figure S9. (a) CLSM images of HeLa cells after being incubated with **BP4** polymersomes for different time periods. The nuclei and endolysosomes were stained with DAPI (blue channel) and LysoTracker red (red channel), respectively. (b) Colocalization ratio analysis between the green channel fluorescence from NBD and the red channel fluorescence of stained endolysosomes. The blue channel was excited at 405 nm and collected between 450-500 nm; the green channel was excited at 488 nm and collected between 510-550 nm; the red channel was excited at 543 nm and collected between 555-595 nm. The scale bars are 25 μm .

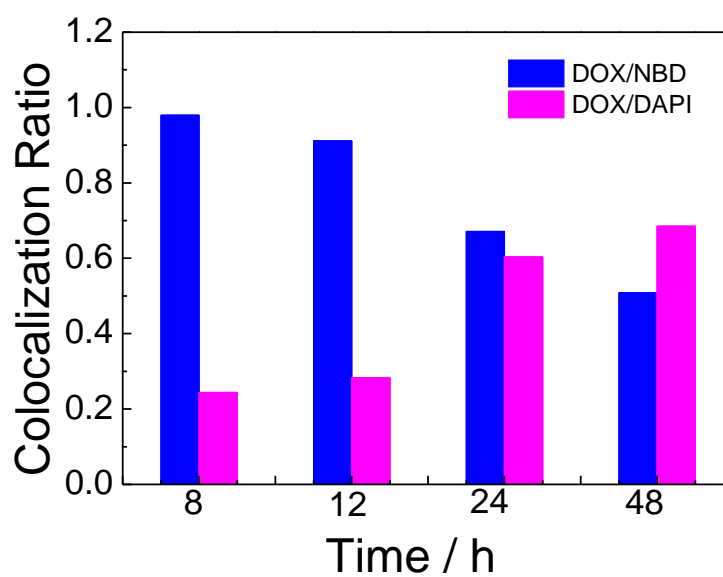


Figure S10. Co-localization ratio analysis on HeLa cells between the red channel from DOX and green channel from NBD and that between the red channel from DOX and blue channel of stained nuclei. The blue channel was excited at 405 nm and collected between 450-500 nm; the green channel was excited at 488 nm and collected between 510-550 nm; and the red channel was excited at 543 nm and collected between 590-650 nm.

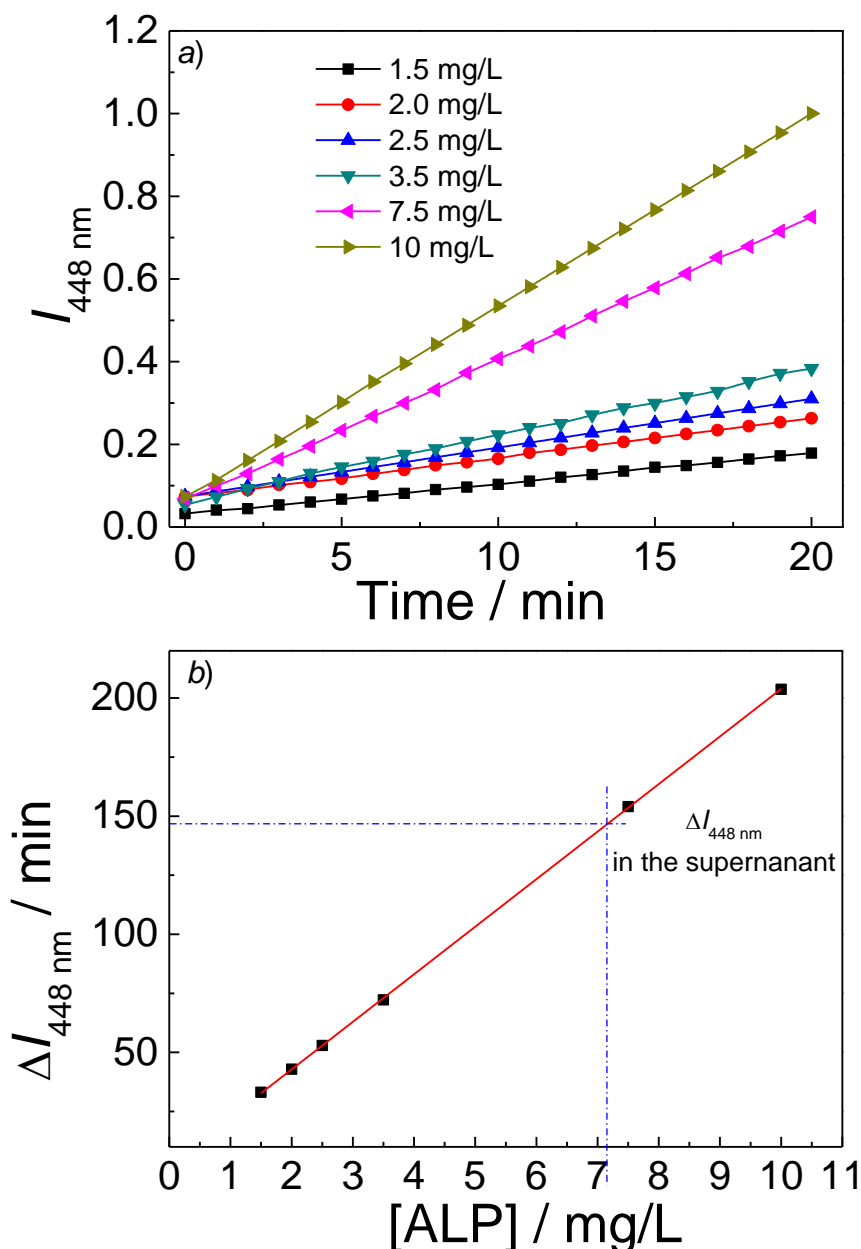


Figure S11. (a) Normalized fluorescence intensity changes at 448 nm and (b) fluorescence intensity change rates ($\Delta I_{448 \text{ nm}}$) of 4-MUP aqueous solution (35 μM) in the presence of varying concentrations of ALP ($\lambda_{\text{ex}} = 400 \text{ nm}$; slit widths: Ex. 5 nm, Em. 5 nm; 37°C). Results are presented as the means \pm s.d. in triplicate.

Note: After ALP encapsulation, the polymersome solution was subjected to ultrafiltration to remove unloaded ALP. After that, the same amount of 4-MUP (35 μM) was added to the supernatant to quantify the unloaded ALP content, which was determined to be 64.4% (wt%) according to the standard calibration curve (Figure S11b). Thus, the ALP loading content was calculated to be 35.6% (wt%).